Supplementary information for

External Fields Effectively Switch Spin Channels of Transition Metals Doped β-phase Tellurene from First Principles

Bin Liu[1, 2, ‡], Jingxian Xiong[1, ‡], Xuefen Kan[3], Sheng Liu[2], Zixin Yang[1], Wenjing Wang[2], Xinxin Zhao[4], Qiang Yu[1, 4*], Sicong Zhu[2, 5*], Jian Wu[1*]

[1] College of Advanced Interdisciplinary Studies, Nanhu Laser Laboratory, National University of Defense Technology, Changsha 410073, China

[2] Hubei Province Key Laboratory of Systems Science in Metallurgical Process, The State Key Laboratory for Refractories and Metallurgy, Collaborative Innovation Center for Advanced Steels, International Research Institute for Steel Technology, Wuhan University of Science and Technology, Wuhan 430081, China

[3] School of Transportation Engineering, Jiangsu Shipping College, Nantong 226010, China

[4] i-Lab & Key Laboratory of Nanodevices and Applications & Key Laboratory of Nanophotonic Materials and Devices, Suzhou Institute of Nano-Tech and NanoBionics, Chinese Academy of Sciences, Suzhou 215123, China

[5] Department of Mechanical Engineering, National University of Singapore, Singapore 117575, Singapore

‡ **These authors contributed equally to this work**

***Corresponding authors: qyu2015@sinano.ac.cn; sczhu@wust.edu.cn; wujian15203@163.com.**

Support information

About MTP methods

All initial configurations are fully relaxed. MTP takes the sum of the contributions of each local atomic environment as the energy of the atom configuration (cfg). $E^{mtp}(cfg)$ is expressed as:

$$E^{mtp}(cfg) = \sum_{i=1}^{n} V(n_i))$$

Where n_i is the atomic environment of the ith atom, the constituent element is composed of its atomic type z_i, which neighbor's atomic type z_j, and its neighbor's position relative to the ith atom z_{ij}. $V(n_i)$ is the local contribution energy of the ith element in its environment, written as:

$$V(n_i) = \sum_{\alpha} \xi_\alpha B_\alpha(n_i)$$

Where ξ_α is the regression parameter of ridge linear regression training, and B_α is the basis function, which is described by the moment tensor:

$$M_{\mu,v}(n_i) = \sum_{j} f_\mu\left(|r_{i,j}|, z_i, z_j\right) \underbrace{r_{ij} \otimes \ldots \otimes r_{ij}}_{v\ times}$$

Where the moment tensors describe the environment of each local atom in terms of radial and angular. $f_\mu\left(|r_{i,j}|, z_i, z_j\right)$ is the radial part. r_{ij} is the angle part. z_i and z_j are atom types for atom n_i and its neighborhood atoms n_j. The radial part consists of two parts, one is the set of radial parameters, and the other is the radial basis function. The radial basis function is a polynomial defined between the minimum interatomic distance in the system and the cut off radius of the neighbourhood where atoms leave (enter) the interaction. $\underbrace{r_{ij} \otimes \ldots \otimes r_{ij}}_{v\ times}$ *is* the angular part, which is the tensor of rank v. When v is 2, the matrix is:

$$r_{ij} \otimes r_{ij} = \begin{pmatrix} x_{ij}^2 & x_{ij}y_{ij} & x_{ij}z_{ij} \\ y_{ij}x_{ij} & y_{ij}^2 & y_{ij}z_{ij} \\ z_{ij}x_{ij} & z_{ij}y_{ij} & z_{ij}^2 \end{pmatrix}$$

Then find the corresponding tensor by the cross product of the matrix, and then get the level of moments ($levM_{\mu,v}$) through these parameters. The coefficients forming the moment level function are generally the optimal solution in experience, and more generally, it is obtained by adding multiple moments ($M_{\mu,v}$). The number of basis function B_α is determined by the threshold of level, and the total number of basis function B_α is further determined. The initial configuration of the training set can be used to determine the fitting

parameters, which can then be used to set up the prediction equation for energy and force prediction. The optimal solution can be searched by[1]:

$$L(\theta^{MTP}) = \sum_{k=1}^{K}\left[w_e\left(E_k^{DFT} - E_k^{MTP}\right)^2 + w_f\sum_{i}^{N}\left|f_{k,i}^{DFT} - f_{k,i}^{MTP}\right|^2 + w_s\sum_{i,j=1}^{3}\left|\sigma_{k,ij}^{DFT} - \sigma_{k,ij}^{MTP}\right|^2\right] \rightarrow min$$

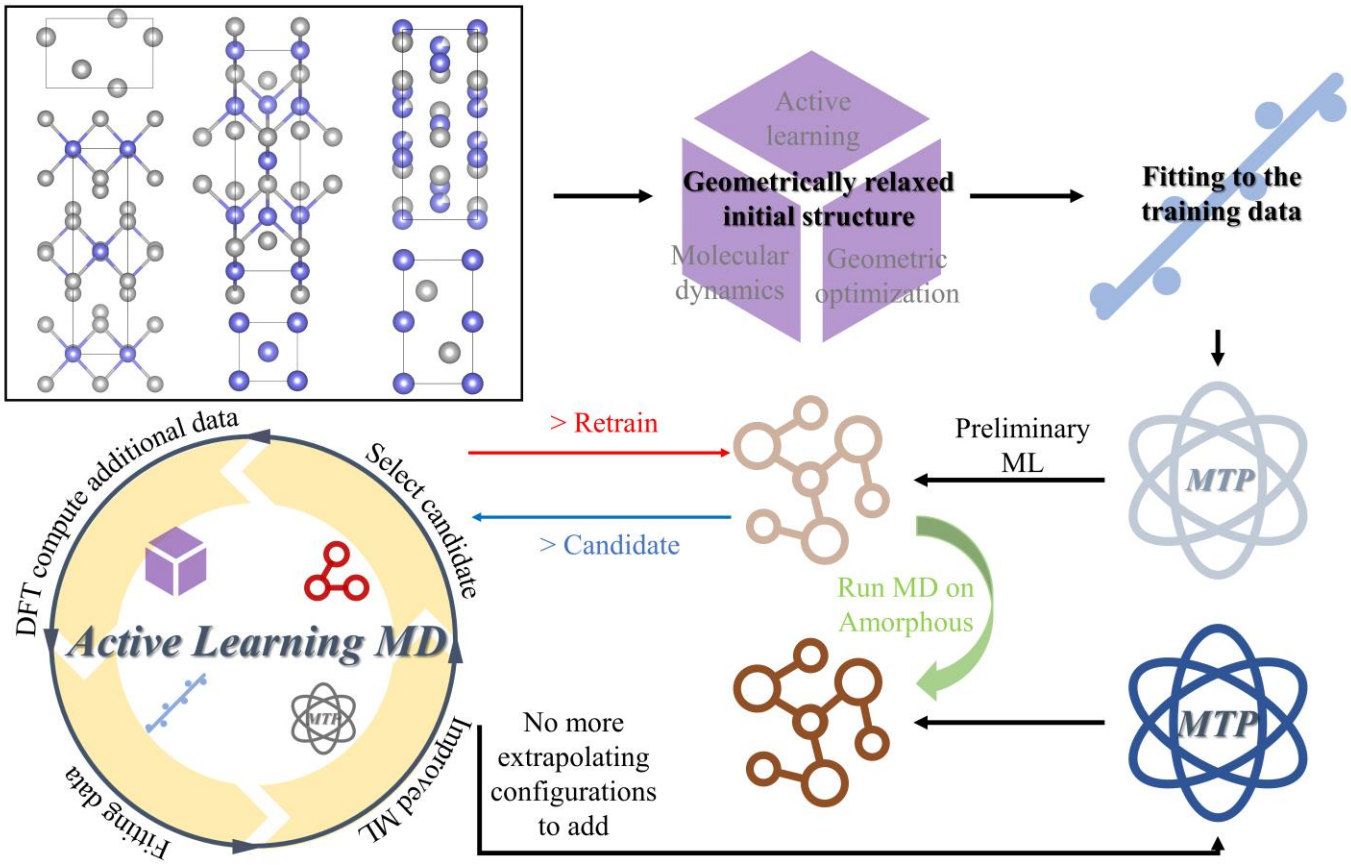

Figure S1. Flowchart for active learning training moment tensor potential (MTP).

MTP training flowchart for TMs-Te is shown in Figure S1 to illustrate the process. The selection of the initial training set is the most basic and important step in the whole MTP training. The structures of all Te and V are selected in Table S1. To ensure the reliability of the initial data, in addition to the original Te and V, AIMD simulation on the remaining 6 structures is carried out, which can be considered as thoroughly optimized data for active learning and training of V-Te MTP. After obtaining the first set of initial data, the active learning strategy was used to simulate the MD of the V-Te amorphous configuration (amorphous $V_{11}Te_{22}$ structure) and improve the initial training data. AIMD has a very high require for computing power, so in the Quantum ATK software package, the reference elements (stress, energy, etc.) in the initial data are calculated by DFT to generate the initial MTP. The initial MTP is used only to generate a new data set and does not require excessive precision. When using the initial MTP for MD simulation, the extrapolation grades (γ) needs to be set.

Extrapolation is a D-optimality criterion generalized to nonlinear cases, which Gubaev describes as an overdetermined equation to concerning θ [2]:

$$E\left(\theta, x^{(i)}\right) = E^{qm}(x^{(i)})$$

If there is an optimal solution, then the left side of the equation is linearized as the Jacobian matrix, and each row of the matrix represents a configuration in the training set.

There are two thresholds are set: candidate (γ_c) and retraining (γ_r). When MD simulation starts, if $\gamma < 1$, then interpolates, if $1 < \gamma$, then extrapolates. If $\gamma_c < \gamma < \gamma_r$, then the configuration is added to the candidate list, if $\gamma_r < \gamma$, then MD is stopped. Configure in the candidate list for DFT optimization, put the optimized structure back into the initial training set, and use the training set added with the new configuration to generate new MTP to assist the next MD simulation. In the TMs-Te system, γ_r is selected as 3 and γ_c as 1. The time length of the MD simulation is 5ps. The MTP in MLIP is used in the Quantum ATK package to generate TMs-Te potential[3, 4].

The doping energy is calculated as follows:

$$E_{Doping} = (E_{TM-doping} + E_{Single-Te}) - (E_{\beta-Te} + E_{TM})$$

Where E_{Doping} is the doping energy of the doping system, $E_{TM-doping}$ is total energy of the doping system, $E_{Single-Te}$ is the energy single atom of Te, $E_{\beta-Te}$ is the energy of primitive β-Tellurene, E_{TM} is the single atom of Transition metal.

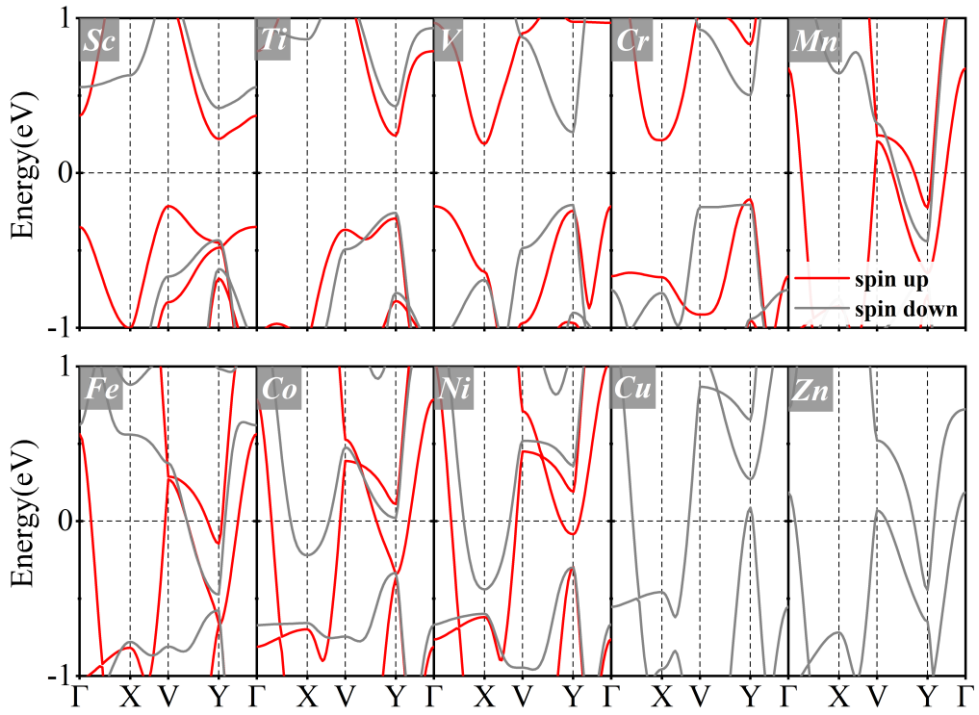

Figure S2. Band structure of the doping system. Band structure after each element substitution. Red indicates spin up, and grey indicates spin down.

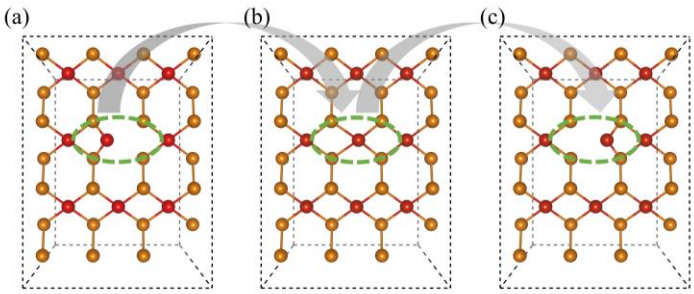

Figure S3. Find the most stable point of V, which is moving from left to right.

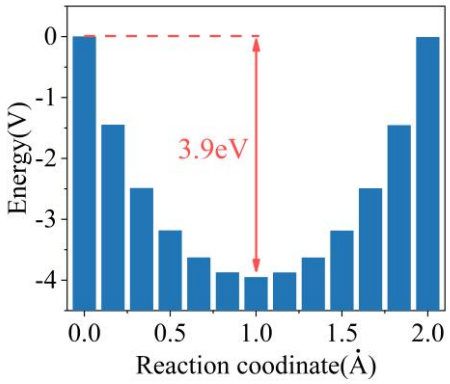

Figure S4. Energy at different moving sites. The energy at the starting position is 0 eV.

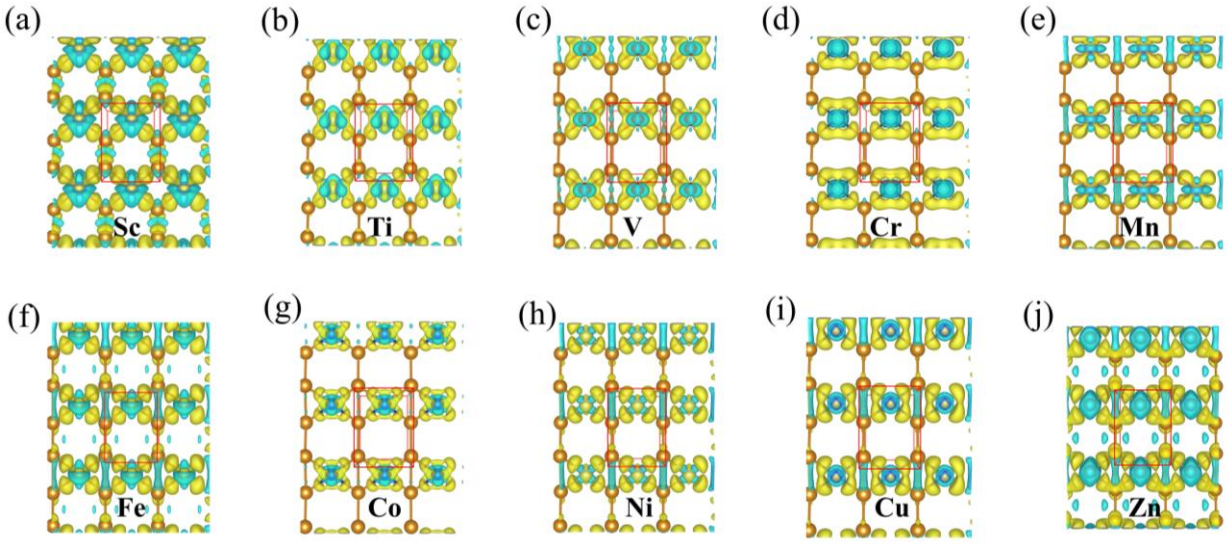

Figure S5. Charge density difference of transition metal replacement Tellurene bridge site.

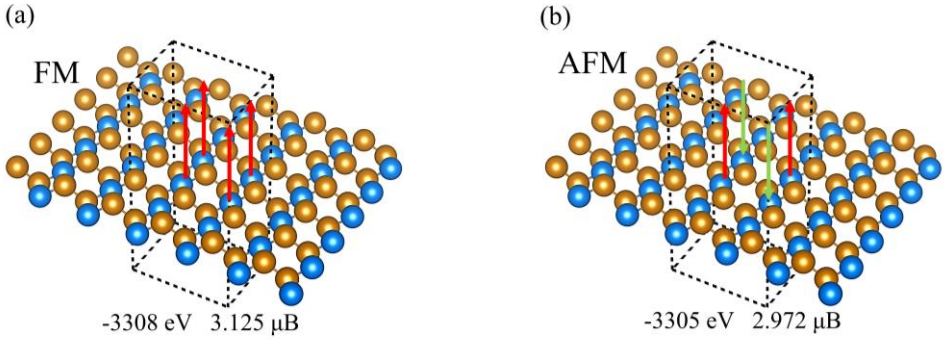

Figure S6. Ground state of V-doping system. We set ferromagnetic and anti-ferromagnetic states in a 2×2 supercell. The magnetic moment of transition metals in ferromagnetic state are all the same, while the magnetic moment of transition metals in the diagonal of the antiferromagnetic state are the same, and the adjacent magnetic moment are opposite. Obviously, the energy of the ferromagnetic state in the V-doped system is -3308 eV, which is lower than that of the anti-ferromagnetic state -3305 eV. Meanwhile, the magnetic moment of anti-ferromagnetic 2.972 μB is lower than that of ferromagnetic 3.125 μB.

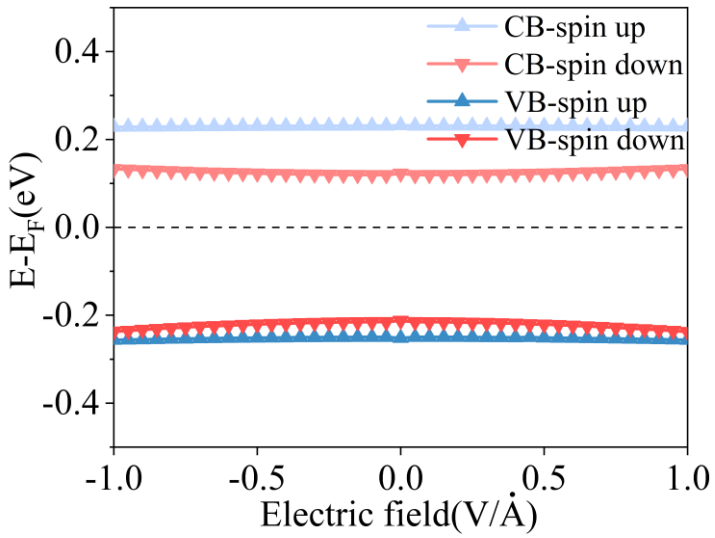

Figure S7. The changes in the conduction and valence bands after the application of the longitudinal electric field. The simulation software we used to calculate the electric field is Quantum ATK.

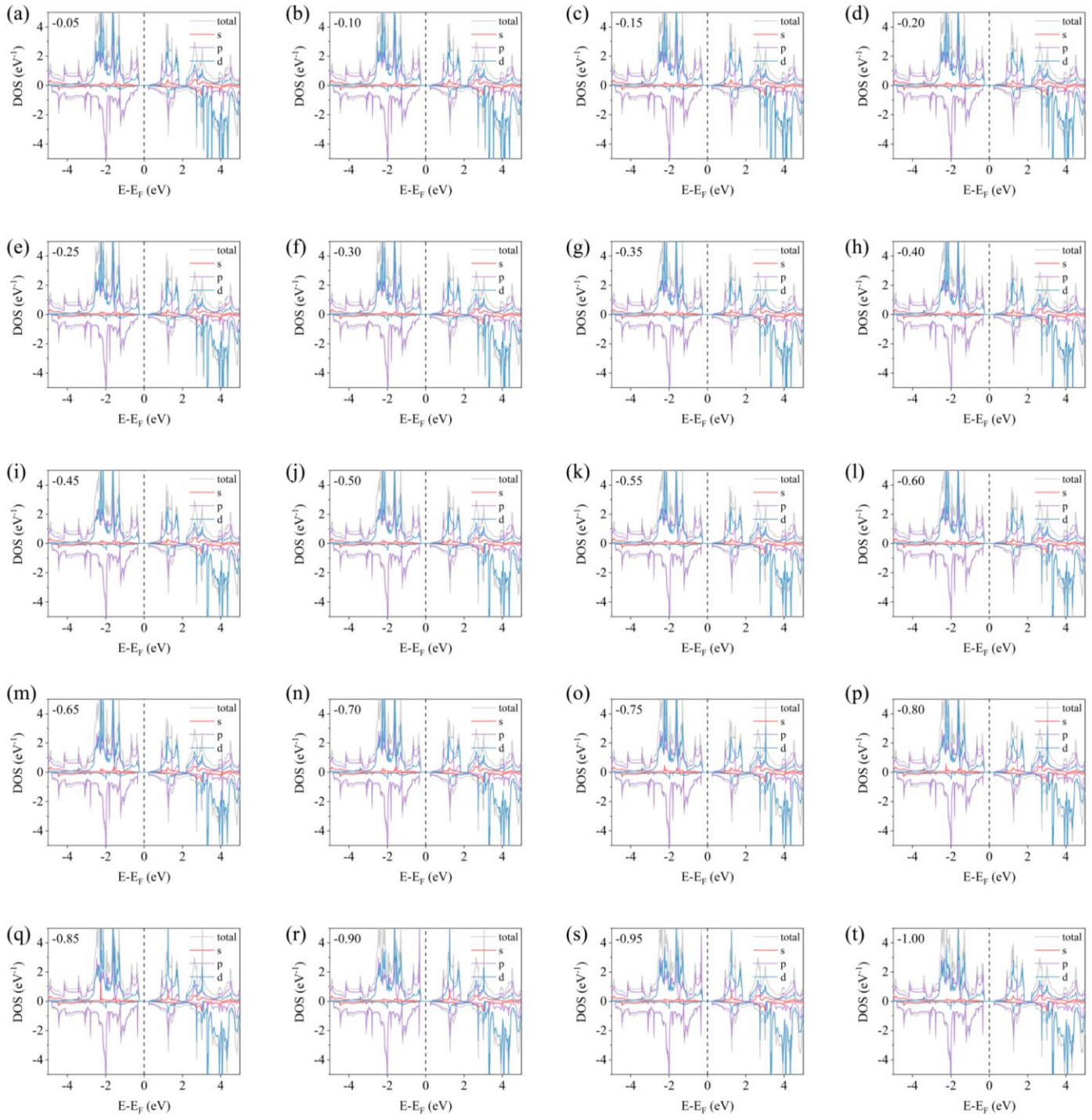

Figure S8. DOS of V-doped system with an electric field ranging from -0.05 to -1V/Å. When Z direction electric field is applied, the DOS hardly changes. The p orbital makes the greatest contribution at the Fermi level. The simulation software we used to calculate the electric field is Quantum ATK.

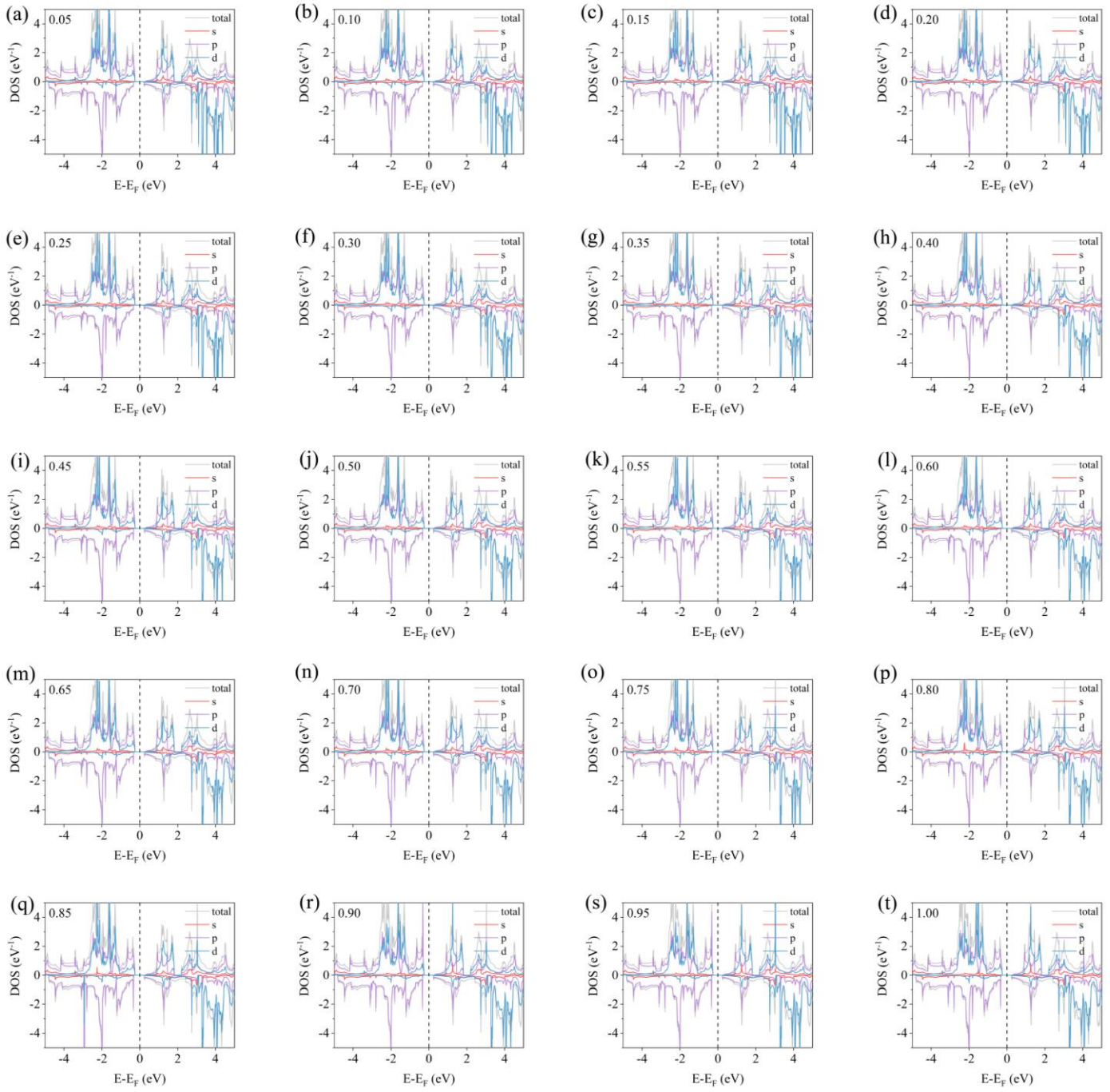

Figure S9. DOS of V-doped system with an electric field ranging from 0.05 to 1V/Å. When Z direction electric field is applied, the DOS hardly changes. The p orbital makes the greatest contribution at the Fermi level. The simulation software we used to calculate the electric field is Quantum ATK.

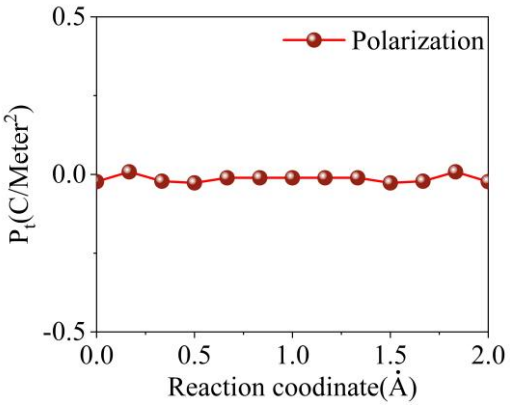

Figure S10. Electrical polarizability at different moving sites. For the V replacement system, the electrical polarization is always maintained at a low level, therefore, the band structure changes little under the application of electric field.

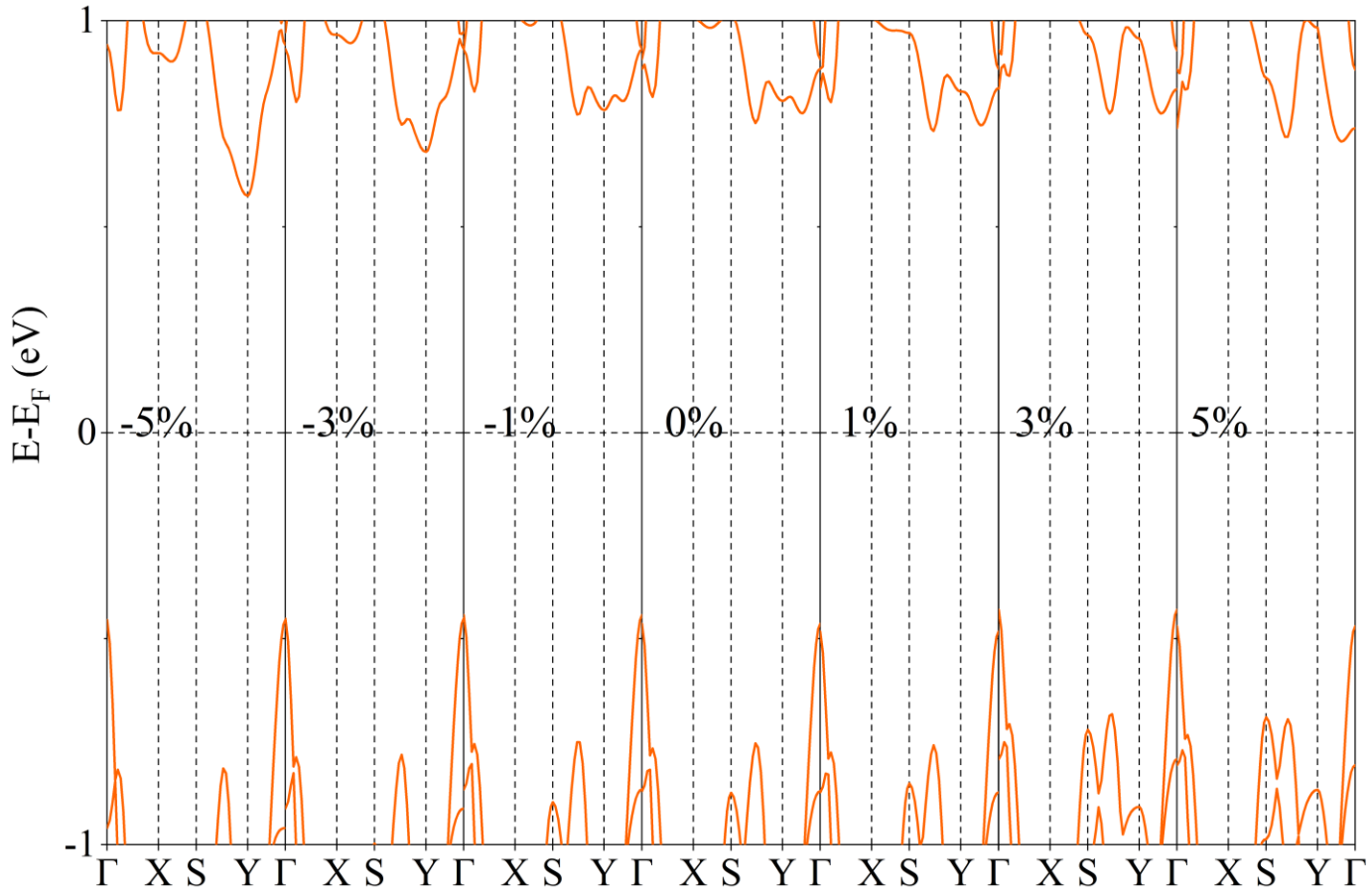

Figure S11. Band structure of β-Te under the strain from -5% to 5%.

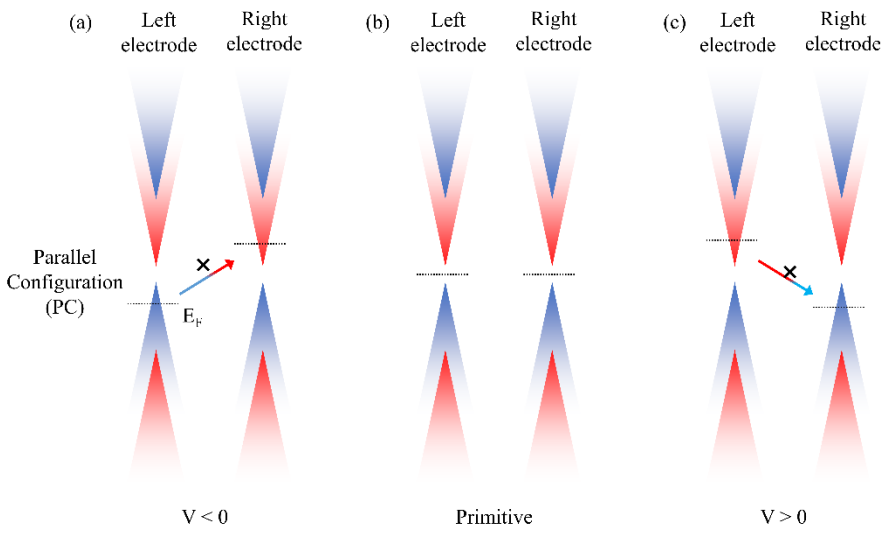

Figure S12. Band structure of two electrodes under different bias in parallel configuration (PC).

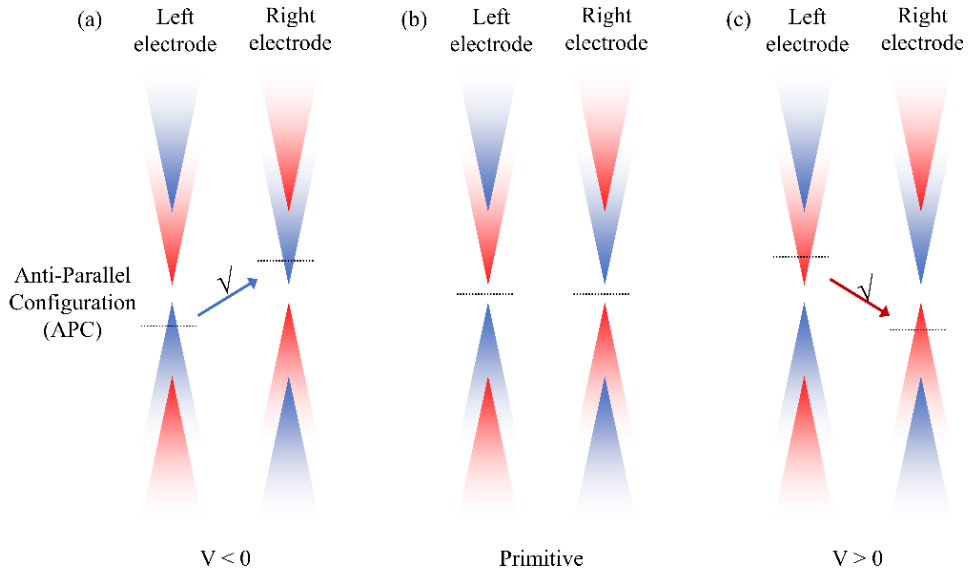

Figure S13. Band structure of two electrodes under different bias in Anti-Parallel Configuration (APC).

In the parallel configuration (PC) as shown in Figure S12, no stable spin transport channel exists in the device, regardless of whether the voltage is less than 0 or greater than 0. However, when the two electrodes are in the anti-parallel configuration (APC) shown in Figure S13, the current under positive and negative bias voltage is contributed by different transport channels.

Table S1. List of initial structures used to build the Te-V MTP training set

Material	**Crystal type**	**Cell volume**	**Space Group**
Te_2V_2	Hexagonal	82.441	186
$V_{1.04}Te_2$	Base-Centered Monoclinic	440.51	12
V_3Te_4	Base-Centered Monoclinic	312.075	12
$V_{4.64}Te_4$	Base-Centered Monoclinic	368.566	12
Te	Hexagonal	101.8	152
V	Body-Centered Cubic	27.758	229

Table S2. Curie temperature (Tc), magnetic moment (M), and effective electron mass (m*) of V doping system under different electric fields. Compared with the original Tellurene system, the effective electron mass is significantly reduced and thus the carrier mobility is significantly increased.

E(V/Å)	Tc(K)	M(μB)	m*(me)	E(V/Å)	Tc(K)	M(μB)	m*(me)
-1.00	160.0	3	0.713	1.00	159.9	3	0.716
-0.95	159.9	3	0.709	0.95	182.7	3	0.710
-0.90	159.8	3	0.703	0.90	182.7	3	0.705
-0.85	159.7	3	0.697	0.85	159.6	3	0.699
-0.80	182.6	3	0.693	0.80	159.6	3	0.695
-0.75	182.6	3	0.688	0.75	159.5	3	0.690
-0.70	151.0	3	0.683	0.70	182.5	3	0.685
-0.65	159.4	3	0.680	0.65	159.4	3	0.682
-0.60	159.3	3	0.676	0.60	159.3	3	0.677
-0.55	159.2	3	0.672	0.55	159.2	3	0.674
-0.50	159.2	3	0.670	0.50	159.2	3	0.670
-0.45	159.1	3	0.666	0.45	159.1	3	0.668
-0.40	182.4	3	0.664	0.40	159.1	3	0.665
-0.35	182.3	3	0.661	0.35	159.1	3	0.662
-0.30	153.0	3	0.659	0.30	159.0	3	0.660
-0.25	159.0	3	0.658	0.25	159.0	3	0.659
-0.20	159.0	3	0.656	0.20	159.0	3	0.657
-0.15	158.9	3	0.655	0.15	158.9	3	0.656
-0.10	158.9	3	0.655	0.10	158.9	3	0.655
-0.05	158.9	3	0.654	0.05	158.9	3	0.654

Table S3. Curie temperature (Tc), magnetic moment (M), effective electron mass (m*), and bader of V doping system under different strain fields (-2% - 5%). Compared with the original Tellurene system, the effective electron mass is significantly reduced and thus the carrier mobility is significantly increased. The Curie temperature decreases gradually with the increase of strain, while the magnetic moment hardly changes. The effective mass of the electron also increases with increasing strain. The bader charge transfer has a very small increase trend with the increase of strain.

Strain(%)	Tc(K)	M(μB)	m*(me)	bader	Strain(%)	Tc(K)	M(μB)	m*(me)	bader
-2.00	155.4	3	0.746	0.9631	3.00	140.6	3	0.560	0.9716
-1.75	154.8	3	0.733	0.9637	3.25	140.2	3	0.553	0.9751
-1.50	154.2	3	0.722	0.9627	3.50	139.5	3	0.547	0.9755
-1.25	153.5	3	0.711	0.9635	3.75	138.8	3	0.540	0.9719
-1.00	169.6	3	0.699	0.9653	4.00	134.2	3	0.534	0.9701
-0.75	152.1	3	0.688	0.9647	4.25	137.3	3	0.528	0.9733
-0.50	151.4	3	0.678	0.9612	4.50	136.5	3	0.523	0.9730
-0.25	150.7	3	0.668	0.9618	4.75	135.8	3	0.517	0.9716
0.25	149.2	3	0.648	0.9677	5.00	134.5	3	0.511	0.9736
0.50	148.4	3	0.639	0.9671					
0.75	156.3	3	0.630	0.9682					
1.00	146.3	3	0.621	0.9710					
1.25	146.2	3	0.613	0.9705					
1.50	145.4	3	0.604	0.9672					
1.75	144.7	3	0.596	0.9662					
2.00	143.7	3	0.591	0.9666					
2.25	143.2	3	0.581	0.9708					
2.50	142.5	3	0.574	0.9718					
2.75	138.1	3	0.567	0.9708					

References

1 ACHAR S K, SCHNEIDER J, STEWART D A. Using Machine Learning Potentials to Explore Interdiffusion at Metal–Chalcogenide Interfaces [J]. ACS Applied Materials & Interfaces, 2022, 14(51): 56963-74.

2 GUBAEV K, PODRYABINKIN E V, HART G L W, et al. Accelerating high-throughput searches for new alloys with active learning of interatomic potentials [J]. Computational Materials Science, 2019, 156: 148-56.

3 NOVIKOV I S, GUBAEV K, PODRYABINKIN E V, et al. The MLIP package: moment tensor potentials with MPI and active learning [J]. Machine Learning: Science and Technology, 2021, 2(2): 025002.

4 SHAPEEV A V. Moment Tensor Potentials: A Class of Systematically Improvable Interatomic Potentials [J]. Multiscale Modeling & Simulation, 2016, 14(3): 1153-73.